DTD 5
ARTICLE IN PRESS

Available online at www.sciencedirect.com
SCIENCE DIRECT®

Physics of the Earth and Planetary Interiors xxx (2004) xxx–xxx

PHYSICS OF THE EARTH AND PLANETARY INTERIORS

www.elsevier.com/locate/pepi

# Electrical imaging of Narmada–Son Lineament Zone, Central India from magnetotellurics

B. Prasanta K. Patro*, T. Harinarayana, R.S. Sastry, Madhusudan Rao, C. Manoj, K. Naganjaneyulu, S.V.S. Sarma

*National Geophysical Research Institute, Hyderabad, India*

Received 19 March 2004; received in revised form 3 August 2004; accepted 3 September 2004

**Abstract**

The Narmada–Son Lineament (NSL) Zone is the second most important tectonic feature after Himalayas, in the Indian geology. Magnetotelluric (MT) studies were carried out in the NSL zone along a 130 km long NNE-SSW trending profile. The area of investigation extends from Edlabad (20°46′16″; 75°59′05″) in the South to Khandwa (21°53′51″; 76°18′05″) in the North. The data shows in general the validity of a two-dimensional (2D) approach. Besides providing details on the shallow crustal section, the 2D modeling results resolved four high conductive zones extending from the middle to deep crust, spatially coinciding with the major structural features in the area namely the Gavligarh, Tapti, Barwani-Sukta and Narmada South faults. The model for the shallow section has brought out a moderately resistive layer (30–150 Ω m) representing the exposed Deccan trap layer, overlying a conductive layer (10–30 Ω m) inferred to be the subtrappean Gondwana sediments, the latter resting on a high resistive basement/upper crust. The Deccan trap thickness varies from around a few hundred meters to as much as 1.5 km along the traverse. A subtrappean sedimentary basin like feature is delineated in the northern half of the traverse where a sudden thickening of subtrappean sediments amounting to as much as 2 km is noticed. The high resistive upper crust is relatively thick towards the southern end and tends to become thinner towards the middle and northern part of the traverse. The lower crustal segment is conductive over a major part of the profile. Considering the generally enhanced heat flow values in the NSL region, coupled with characteristic gravity highs and enhanced seismic velocities coinciding with the mid to lower crustal conductors delineated from MT, presence of zones of high density mafic bodies/intrusives with fluids, presumably associated with magmatic underplating of the crust in the zone of major tectonic faults in NSL region are inferred.


*Keywords:* Magnetotellurics; 2D inversion; Narmada–Son Lineament

## 1. Introduction

The Narmada–Son Lineament (NSL) is a zone of weakness since the Precambrian times. Areas to the north and south of NSL experienced vertical block

* Corresponding author. Tel.: +91 40 23434700; fax: +91 40 27171564.
*E-mail address:* patrobpk@rediffmail.com (B.P.K. Patro).

0031-9201/$ – see front matter © 2004 Elsevier B.V. All rights reserved.
doi:10.1016/j.pepi.2004.09.001

movements (West, 1962). Auden (1949) reported that NSL is a subcrustal feature influencing the deposition and folding of the Vindhyans (Meso-Neoproterozoic) and Gondwanas (Permo-Carboniferous-lower Cretaceous). The exposed older Bijawars along the margin of Vindhyan basin indicate uplift of the basin boundaries followed by sinking along the central axis of the basin during Vindhyan sedimentation (Krishnan and Swaminath, 1959). Narmada valley represents a zone of tectonic truncation of regional structural trends and is bounded by the Narmada North and Narmada South fault (NSF) systems (Acharya et al., 1998). Major movements such as uplift, subsidence and transcurrent motion ceased at the end of lower Proterozoic. However, there were recurrent tensile reactivations leading to gravity faulting. High heat flow (Shanker, 1988; Roy and Rao, 2000) thermal activity as indicated by sulphur springs (Gupta and Sukhija, 1974), and continuing seismicity (Rastogi, 1997) point out to recent tectonic activity in the Narmada–Son region. From the seismotectonics point of view, the NSL region is known to be a significantly disturbed zone. The 6.0 M Jabalpur earthquake of 22 May 1997 is associated with the Narmada South fault. Similarly the NSF passes through Khandwa located at the northern end of the present MT traverse from where a significant episode of seismic tremor activity was recently reported (http://www.gsi.gov.in/khandwa.pdf).

Fig. 1 presents the geology along with major structural features of the NSL zone. Graben and horst structures with boundary faults trending roughly parallel to the NSL strike is a characteristic pattern of subsurface structure in the NSL zone. In the north, the Narmada valley region is highly disturbed and a

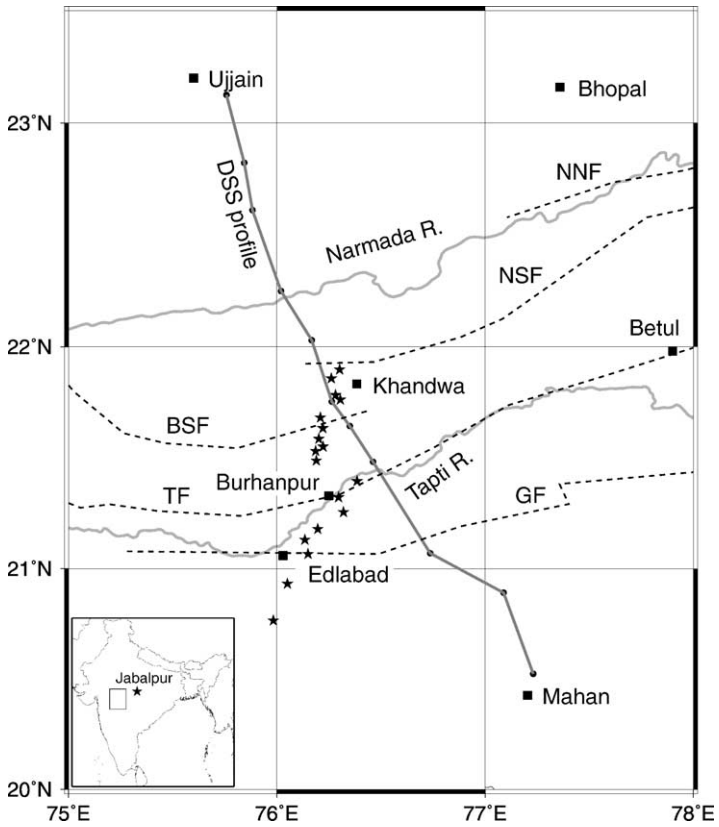


Fig. 1. Location of the MT stations (marked as star) and the tectonics of the study area (Crumansonata, 1995). Ujjain-Mahan deep seismic profile is also plotted. NNF: Narmada North fault; NSF: Narmada South fault; BSF: Barwani-Sukta fault; TF: Tapti fault; GF: Gavligarh fault. Inside the key map the epicenter of Jabalpur earthquake ($M = 6.0$) is marked as star.

series of E–W/ENE–WSW trending faults have been recorded. The Narmada–Tapti region is dissected by several faults—the major ones being Narmada South fault (NSF), Barwani-Sukta fault (BSF), Tapti fault (TF) and Gavligarh fault (GF). Narmada South fault and Barwani-Sukta fault, the two major structural features traverse in an E–W to ENE–WSE direction passing through Khandwa region in the northern half of the study area. Further south, the Tapti fault, starting from west of Anakdev extends upto Burhanpur with a series of NS cross faults continues towards Betul. Another fault popularly known as Gavligarh fault starts from north of Edlabad in Purna valley and extends along the alluvium contact towards Seoni.

Several geophysical studies were carried out in the NSL region to investigate the nature of crust and upper mantle particularly in respect of density and velocity structures and related features of crust–mantle interaction. The Bouguer gravity map of the Narmada–Son region, compiled utilizing the data sets collected during CRUMANSONATA programme (Rao et al., 1982; Rao and Sastry, 1986) and during the Upper Mantle Project (Kailasam, 1979), shows several high amplitude with long as well as short wavelength anomalies covering the NSL region all along its length. While some of the major gravity lows have been attributed to known sedimentary basins, viz. Vindhyans, Gondwanas, the gravity highs are interpreted in terms of heavier subsurface basic bodies in the crustal column (Verma and Banerjee, 1992). Five deep seismic sounding (DSS) traverses cutting across the NSL region were occupied and the results brought out anomalous crustal structure with the lower crust characterized by velocities in the range 7.0–7.5 km/s. These are interpreted in terms of transitional zone (Kaila et al., 1985). The DSS results along the Ujjain-Mahan profile, in the western part of NSL indicate upwarping of Moho in the area. The depth section along Ujjain-Mahan reveals a block structure of the crust, with individual blocks bounded by deep faults extending almost to Moho (Fig. 2). Major tectonic adjustments in various crustal blocks, in this region, occurred in Precambrian/Gondwana times. The observed reverse block movements during Precambrian and Gondwana times and existence of shallow sedimentary basins below Deccan traps, point out to the presence of deep seated tectonic activity in this region, which must have been responsible for the formation of Vindhyan and Gondwana sedimentary basins.

Earlier MT measurements, covering a frequency range of 100–0.01 Hz were carried out along a 100 km long traverse in the Satpura range and Tapti basin in the Khandwa region helped bringing out thickness variations of trap as well as the subtrappean Gondwana sediments along this traverse. Two-dimensional (2D) forward modeling of MT data along this profile indicated possible presence of a wide conductive zone extending from shallow depths of about 3–4 km, down to lower crustal levels and this has been interpreted to be a fluid filled fractured upper crustal block lying in the middle of the traverse (Rao et al., 1995). Another MT study based on measurements along a 350 km long MT traverse from Rajnandgaon to Bareli cutting across the NSL revealed an electrical block structure with differing block resistivities. The high resistive upper crust overlying a conductive lower crust, is shown to be thick approximately 20 km at the southern end of traverse falling in the crystalline shield region and becomes thinner and thinner as the traverse enters the NSL region (Sarma et al., 1996). GDS studies (Arora et al., 1995) indicate a crustal conductor located south of Jabalpur, in the NSL region. Results from MT study by Gokarn et al. (2001) in the NSL region delineated two conductive features of about 30 Ω m in a depth range between 10 and 35 km. They interpreted that high conductivity is due to fluids present in the fractures associated with the fault. Rao et al. (2004) identified two conductive bodies (10–200 Ω m) in the Khandwa region and interpreted the conductor observed below the Narmada graben in terms of partially molten magma emplaced in the crust from asthenosphere levels.

Though geophysical studies conducted earlier in the NSL region provided valuable data sets and concepts on subsurface features (Mishra et al., 2001), keeping in view of the vast seismotectonic significance of the NSL zone in general and the Khandwa area in particular, an MT study has been undertaken. The main objective of this study was to delineate the subtrappean sediments (if any), characterization of the crustal geoelectrical structure and to examine the nature of electrical signatures of the known faults. The present MT traverse extends from Edlabad to Khandwa and cut across major structural features like the NSF, BSF, TF and GF (Fig. 1). It passes through the major gravity anomalies near Khandwa and Burhanpur. The Ujjain-Mahan DSS traverse is located close to the MT traverse.

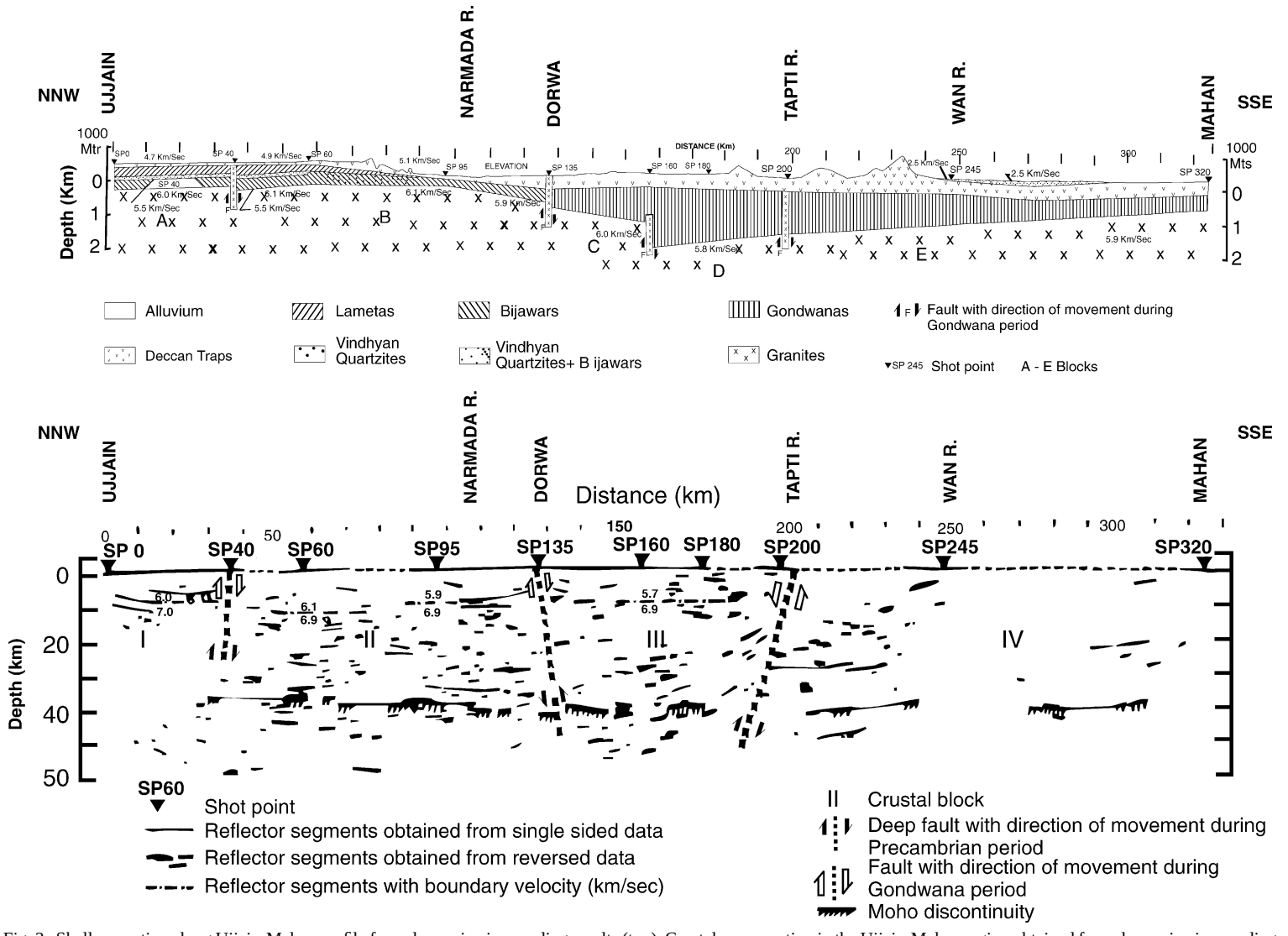


Fig. 2. Shallow section along Ujjain-Mahan profile from deep seismic sounding results (top). Crustal cross-section in the Ujjain-Mahan region obtained from deep seismic sounding results (Kaila et al., 1985) (bottom).

## 2. The data

MT data were recorded with a GMS05 system (M/s. Metronix, Germany) in the frequency range 0.001–1000 s. The two horizontal electric field components were acquired, on two orthogonal dipoles of 80–90 m length, with porous pot electrodes containing $CdCl_2$ electrolyte and Cd core. The horizontal and vertical magnetic field components were measured with induction coil magnetometers. MT measurements were carried out during 1999 along Edlabad (in the south)–Khandwa (in the north) profile oriented in NNE-SSW direction. The profile extends over a length of 130 km. In this region intense seismic tremor activity has been reported recently (Mishra et al., 2001). A total of 18 soundings were carried out with station spacing ranging from 5 to 20 km, with wider station spacing in the southern half of the traverse. Since the area north of Edlabad is electrified with high tension power lines and occupied by irrigated lands, more effort had been made, for selecting reasonably good MT sites. Small deviations from the original planned traverse had to be made in the case of EK11, EK12 and EK13, where eastward shifting of sites had to be done. The traverse passes through mainly over the Deccan trap terrain while it goes into an alluvium cover at its southern end.

All the data were processed using PROCMT (Metronix, Germany) software package. This processing facilitates robust single site estimates of electromagnetic transfer functions. Prior to conversion into the frequency domain the time series data of each of the electric and magnetic field components was manually edited by identifying and rejecting the bad segments containing spikes. The MT impedance tensor and the two magnetic transfer functions were calculated using the regression of M-estimate. Unfortunately at most of the sites vertical magnetic field (Hz) data was noisy and therefore it was not considered for analysis.

To start with, a general qualitative assessment of geoelectric character of the subsurface along the traverse is attempted through an examination of MT apparent resistivity and phase pseudosections of the off-diagonal elements of the rotated impedance tensor corresponding to the TE and TM modes (Fig. 3). From the strike analysis carried out we derive the strike direction as N75°E as discussed in Section 3.

The prominent features of the data, identified from Fig. 3 are as follows. In the higher frequency range (100–4 Hz), a low resistive layer may be seen in the southern half of the profile. This layer represents the alluvium cover resting on the Deccan trap layer which in turn overlies a more resistive granitic basement. In the middle of the traverse (sites EK11–EK17) the top layer, characterized by moderate resistivities represents the Deccan trap cover. However, towards north, near Khandwa, the top surface becomes conductive again representing alluvial cover. Beneath the NSL zone at longer periods a good conductor can be observed in TE mode. This is in good agreement with the phase psuedosections. Possible static shift effects were indicated only at a few stations, e.g., at EK12.

## 3. Dimensionality of MT transfer functions

A consistent regional strike direction for the whole profile or at least for some parts of it has to be determined before considering any 2D modeling or inversion. As a first step, we investigate the dimensionality of the data. For this purpose, Swift's (1967) non-dimensional invariant parameter 'Skew', which measures the departure from an ideal 2D model, has been used. In the case of a perfect 2D earth the skew will be zero, while skew values greater than 0.1 may be taken as indicators of a 3D structure or galvanic 2D model. Fig. 4 (top) shows the contour plot of Swift's skew parameter for the profile, as a function of period. The values are generally small (<0.1) for periods upto 100 s supporting the assumption of a 2D earth. At a few stations higher skew values are observed at longer periods are observed at some of the sites, for e.g., EK14, EK15, EK24. Fig. 4 (bottom) shows the contour plot of phase sensitive skew (Bahr's skew) values. A phase-sensitive skew can be determined from the consideration that in a regional 2D structure the column elements of impedance tensor must have the same phase (Bahr, 1988; Bhar, 1991). The Bahr's skew values (Fig. 4, bottom) are mostly below 0.3. The empirically determined threshold for Swift skew is 0.2 and that for Bahr skew is 0.3, above which the 2D assumption is not valid (Bhar, 1991). However, in many situations the low skew need not necessarily represent a 2D earth since some 3D structures can also show small skew values (Ting and Hohmann, 1981).

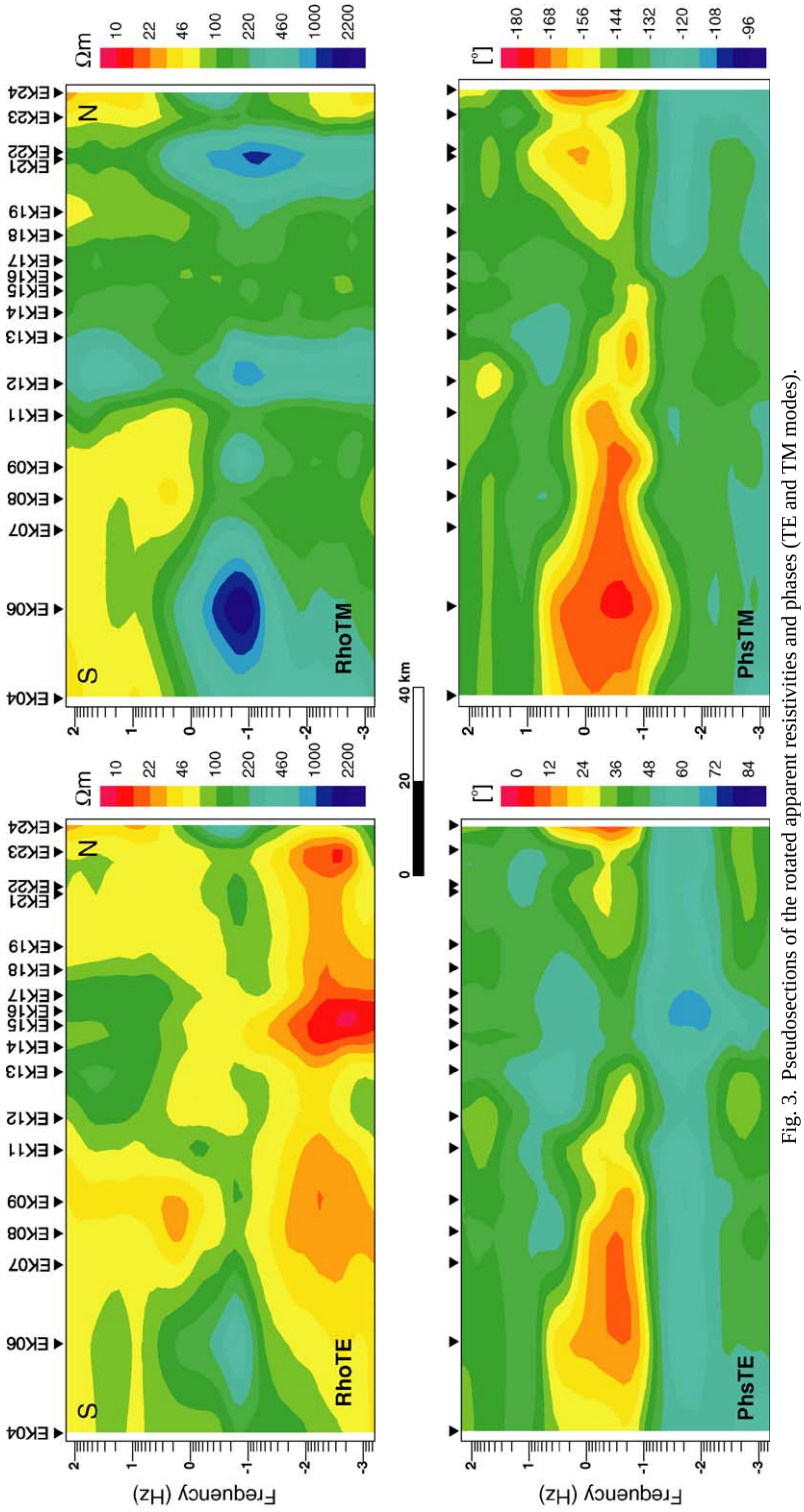


Fig. 3. Pseudosections of the rotated apparent resistivities and phases (TE and TM modes).

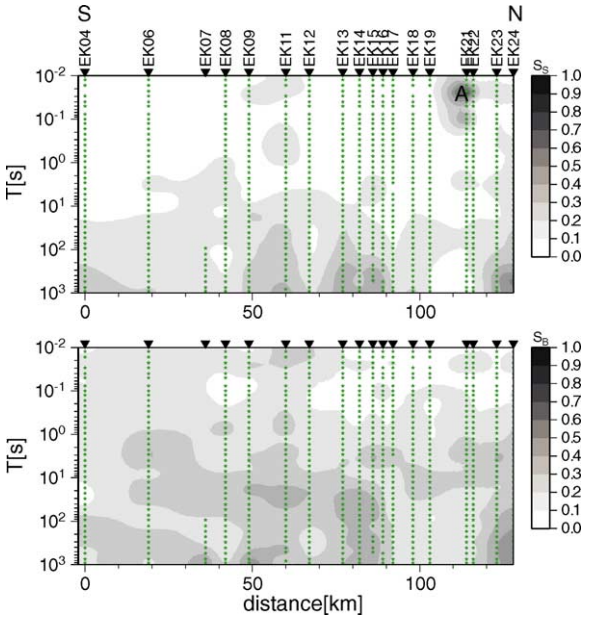


Fig. 4. Contour plot of Swift skew (Swift, 1967). High skew values at EK21, marked 'A' are due to bad data quality in the high frequency range (top). Contour plot of phase sensitive skew (Bahr, 1988) (bottom).

In the present case the geological structure in the NSL zone is controlled by major tectonic features with well defined strike (close to E–W direction).

The geoelctric strike direction was calculated using tensor decomposition techniques of Smith (1997) and Becken and Burkhardt (2004) for the period range 0.1–100 s (shown in Fig. 5). Smith's analysis incorporates different parameterization of the distortion matrix and allows for the distortion model to be fitted either to individual periods or to a period band at each site. The best strike derived from Smith's analysis was W70°N (N70°E). Necessary conditions for the presence of a regional 2D structure (no matter whether galvanically distorted or not) are linear polarization states of the horizontal electromagnetic fields in principal coordinates assuming a linearly polarized primary magnetic field. This fact is used in the analysis of the impedance tensor of Becken and Burkhardt (2004). They show, that such linear polarization states of the horizontal electric and magnetic fields produce linearly polarized columns (i.e., the telluric vectors) of the impedance tensor. The polarization states and thus the ellipse parameters used in the decomposition of Becken and Burkhardt (2004) are rotationally variant. If a coordinate system can be found, in which the ellipticities of both the telluric vectors vanish identically, linear polarization and thus a regional 2D structure is assumed. Otherwise, the presence of a 3D structure is to be considered. In the case of a 2D structure, the parameters of the ellipse are related to the principal impedances and the distortion angles used by Smith (1995). Apart from a different treatment of error bars, the results should be identical to those of other distortion analyses. In practice, however, data have always at least small 3D contributions. In such cases, the analysis of Becken and Burkhardt (2004) might be advantageous, because they use a full eight parameter description of the impedance tensor (in contrast to the classical seven parameter distortion analysis) and thereby avoid possible bias of the strike angle estimate and/or impedances and distortion parameters. The strike direction derived for the present data, in the period range 0.1–100 s is relatively consistent N75°E (Fig. 5). The behavior of ellipticities ($\varepsilon$) and the distortion angle ($\alpha$) as a function of period for the site EK17 is presented in Fig. 6. The distortion angles are very small indicating rather a low degree of distortion in the study area. The ellipticites approximately vanish in this period range and the orientation of telluric vector is found to be independent of period. Thus, 2D analysis seems to be permitted. Deviations of ellipticities from zero are explainable by data errors as can be deduced from error bars in Fig. 6.

Considering the consistency of the results from both the analyses and also because of the estimated strike being in agreement with the Geological strike (ENE–WSW to EW), we have rotated the data to N75°E and assigned the *xy* component to the E polarization (or TE mode), where the electric field is transverse to the lateral conductivity contrast (parallel to the strike) and the *yx* component to B polarization (or TM mode), where the magnetic field is transverse to the lateral conductivity contrast (parallel to the strike).

## 4. Modeling results

### 4.1. Shallow crustal section

The high frequency (1000–1 Hz) data were inverted using the rapid relaxation inversion (RRI) algorithm of Smith and Booker (1991) to get the shallow sec-

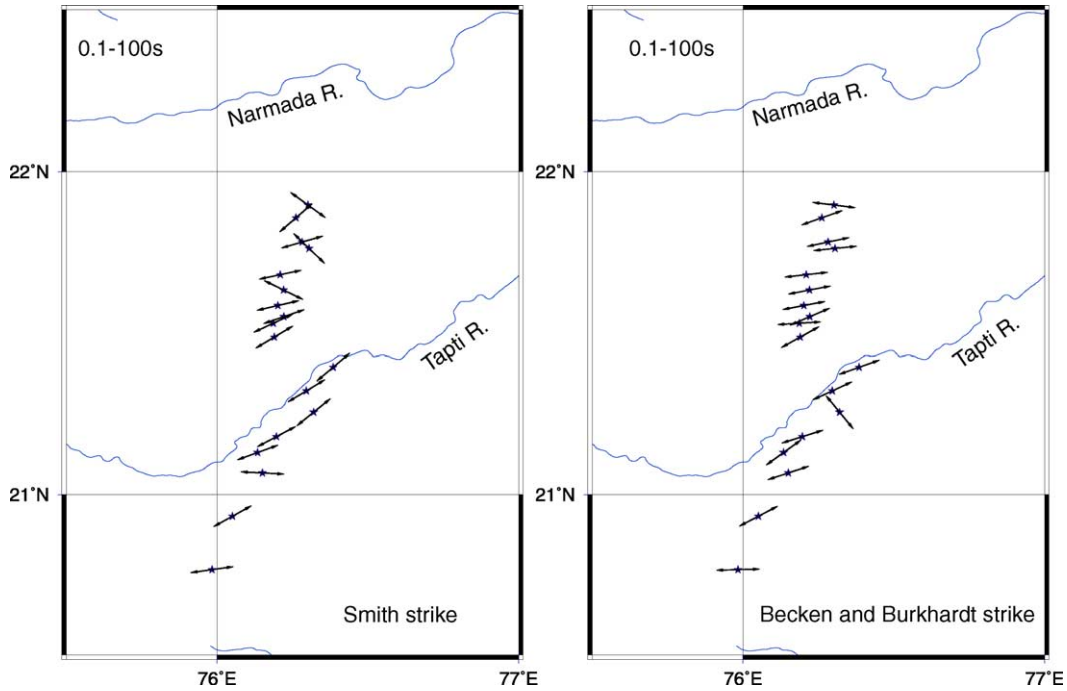


Fig. 5. The geoelectric strike direction calculated using the tensor decomposition technique of Smith (1997) and Becken and Bukhardt (2004) for the period range of 0.1–100 s.

tion. The site EK7 was not included in the inversion due to bad data quality in the high frequency range. The inversion was started from an initial model based on a stitched 1D layered section along the traverse. By systematic trials, an optimal value for the weighing factor "$\alpha$" was estimated which amounts to 8. With this value of $\alpha$, after 15 inversion steps, followed by 20 smoothing steps, the data misfit converged and the model roughness is found to decrease slowly. The final rms misfit for TE mag, TE phase, TM mag and TM phase are 6.329, 7.224, 5.036 and 8.035, respectively. Fig. 7 shows the final model obtained and the fit between observed and computed response curves at a few sites. The results clearly bring out a model for shallow section comprising a top moderately resistive layer (30–150 Ω m) representing the Deccan trap layer and an underlying conductive layer (10–30 Ω m) corresponding to subtrappean Gondwana sediments. The trap thickness ranges between 0.8 and 1.2 km while the thickness of underlying sediments varies from 0.5 to 1 km between EK4 and EK11 covering the southern half of the traverse. A sudden thickening of sediments (∼2 km) below a thick trap layer (∼2 km) in the middle of the traverse between sites EK11 and EK19, indicates a subtrappean sedimentary basin like feature. This feature is clearly brought out from the present 2D model and agrees closely with the 1D section (Patro, 2002). A sharp decrease in the thickness of the trap cum sedimentary column may be seen at site EK19, apparently marking the northern boundary of this basinal feature. Further north along the traverse, a thin (200 m) surface layer of resistivity 20–40 Ω m is observed. This layer corresponds to alluvium that covers the Deccan trap layer.

### 4.2. Deep crustal image

The 2D inversion code of Rodi and Mackie (2001) implemented in WinGlink package was used to jointly invert E and B polarization resistivites and phase in the period range 0.001–546 s. This code computes regularized solutions of 2D magnetotelluric inverse problem by employing a nonlinear conjugate gradients (NLCG) scheme to minimize an objective function that penal-

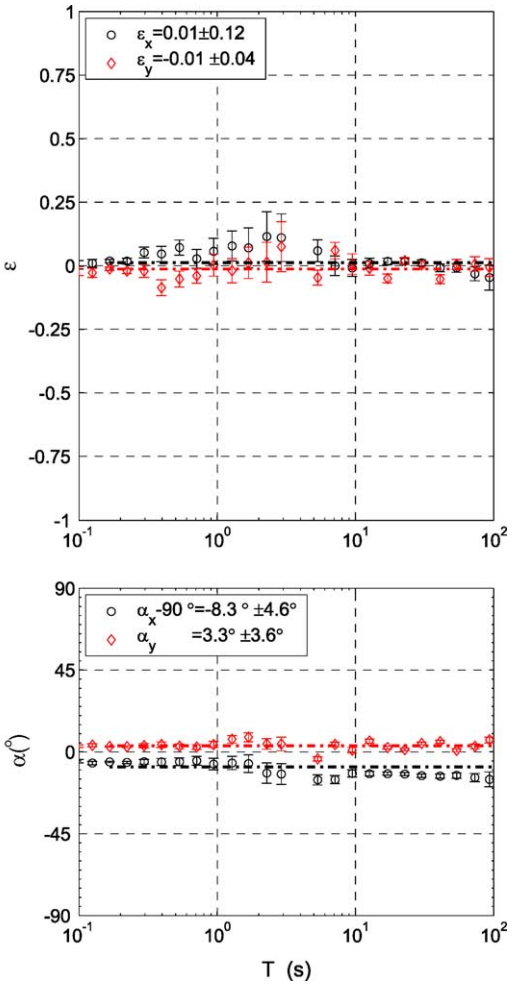


Fig. 6. Plot of ellipticities ($\varepsilon$) and the distortion angle ($\alpha$) as a function of period for the site EK17.

izes data residuals and second spatial derivatives of resistivity. The behavior of the inversion process is mainly controlled by a trade-off parameter "$\tau$" representing a measure of compromise between data fit and model smoothness. To find a suitable value for "$\tau$" an L-curve (Hansen, 1998) is plotted between model roughness and rms error (Fig. 8). The value corresponding to the corner of the curve (in this case $\tau = 10$) is considered as most appropriate for the model. The inversion was started from a homogeneous half space of 100 Ω m. An error floor of 20% for apparent resistivity and 1.5° for phase is assigned, thus downweighing the apparent resistivity with respect to the phase. This in turn helps minimizing the static shift effect in the principal apparent resistivities. This will also yield a smooth model with better data fit in phase while there may be deviations in apparent resistivity. A smooth model is obtained after 150 iterations, where data misfit converged to a plateau. From the numerical experiments it was demonstrated that in early stages of the inversion process substantial information may erroneously be transferred to static shifts (Brasse et al., 2002), hence the static shift effects were corrected from the responses of final model. The inversion output after 15 iterations is shown in Fig. 9.

The model brings out four highly conductive features (A–D) extending vertically from middle to deep crustal levels, characterizing the subsurface along the traverse. These conductive features presumably representing fracture/fault zones cut across the high resistive crustal column and are seen to be spatially coincident with known tectonic faults in this area. The features "B" and "C" correspond to Tapti and Barwani-Sukta faults, respectively. Similarly, the features "A" and "D" are inferred to be the electrical signatures of the Gavligarh fault located at the southern end of the traverse and the Narmada South fault at the northern end of the traverse, respectively. The lower crustal column is relatively conductive. The root mean square (rms) error for all the sites and the data fit at some representative site is shown in Fig. 10. The sensitivity plot (Fig. 9) shows four regions of high sensitivity that correlate with the regions corresponding to the four conductive features modeled. These features are therefore well resolved which means that small changes of model parameters have large effect on model response. Even in this, the regions of high conductivities located in the central portion in the postulated fracture zones may be considered to be relatively more resolved (yellow to red, sensitivity >1) as compared to the region below (green, sensitivity 0.1–1). To examine the model further, in particular the resolution of the conductive features, the MT data was also modeled independently (Patro, 2002) with the inversion code of Smith and Booker (1991). The high conductive features were found to be well resolved with comparable depths and conductivity values.

In order to test the necessity of the conductive features A–D, forward responses were calculated with and without the respective conductive features in the model. Fig. 11 shows the forward response (both for apparent resistivity and phase) of the model with and without the

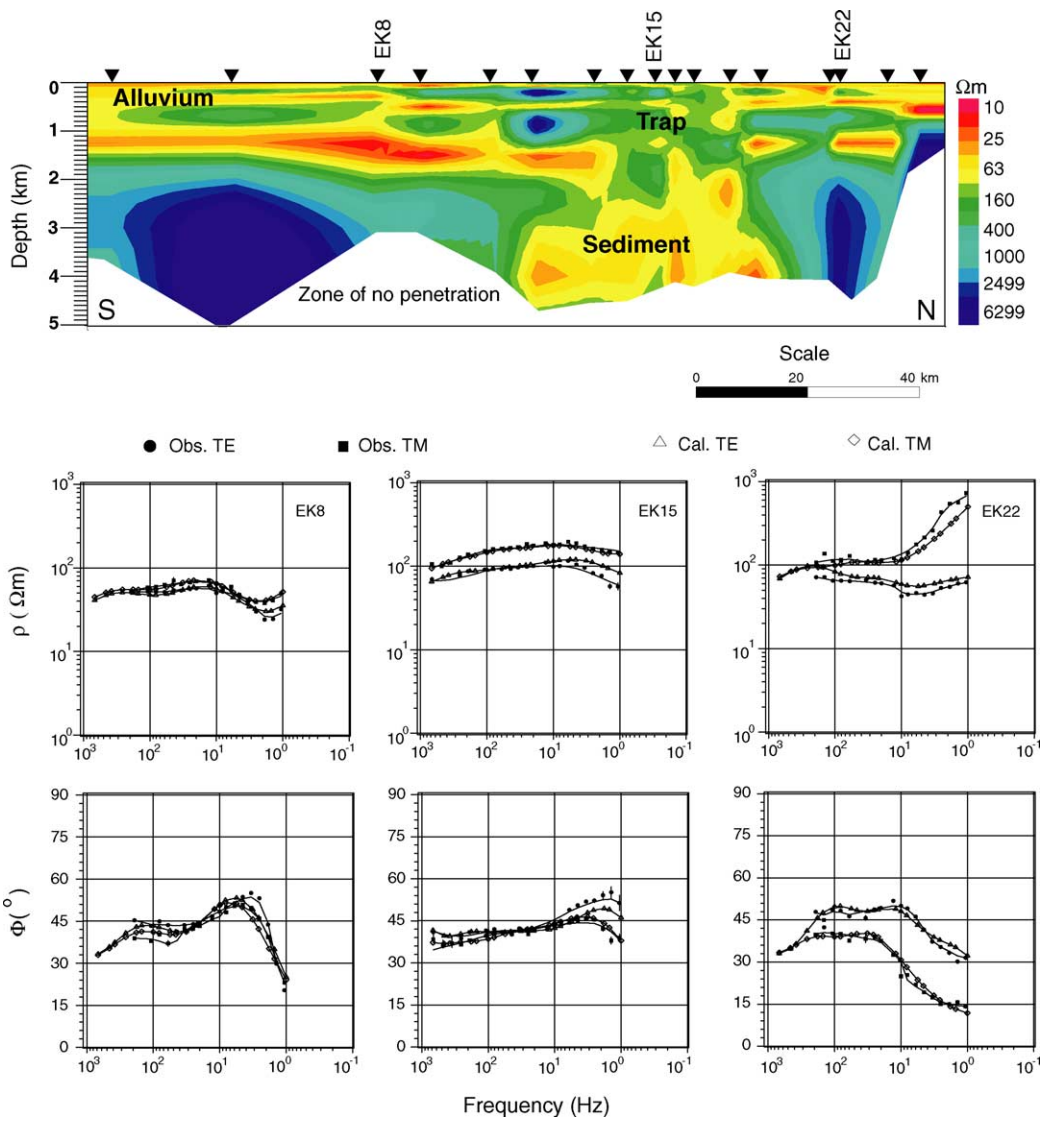


Fig. 7. Shallow geoelectric cross-section obtained from 2D inversion using rapid relaxation inversion scheme of Smith and Booker (1991) (top). Zones of no penetration are blanked out. Fit with the observed and computed responses at few sites (bottom).

conductive feature 'C' plotted along with the observed response. The modeling results clearly support the necessity of the presence of conductive features (A–D) in the model.

Besides the 2D model presented above, another possible candidate that might equally explain the observed responses of the magnetotelluric data, particularly the split in apparent resistivity and phase data at long periods, is anisotropy. The conductive features (A–D) derived from the above 2D isotropic modeling study could also be modeled as an image of an anisotropic block. Heise and Pous (2001) demonstrated from synthetic data set (generated from anisotropic model) that, if the same is analysed with an isotropic inversion scheme, it could give rise to a model comprising of dyke like structures. Directional dependence of the electrical conductivity as is observed at neighboring sites, could also be modeled by lamellae (Bahr et al., 2000). However,

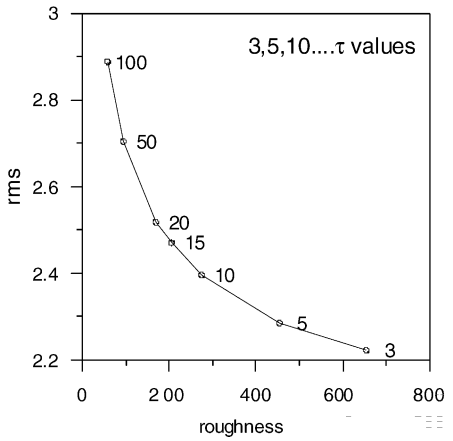


Fig. 8. To determine the optimal trade-off parameter the rms was plotted against model roughness resulting in a typical L-form (Hansen, 1998). An optimal trade-off parameter we choose $\tau = 10$.

these possibilities are not dealt in this paper but provide scope for further research.

## 5. Comparison and integration of magnetotelluric, deep seismic sounding and gravity results

Though there is considerable deviation between the location of MT and nearby Ujjain-Mahan DSS traverses, they come close to each other in the middle of the MT traverse (see Fig. 1). Comparison of MT section with the seismic modeling results of the Ujjain-Mahan DSS traverse brings out a close agreement between the two. Particularly the subtrappean sedimentary basin identified in MT section between the sites EK11 and EK19 finds an expression in the DSS section in the form of a subtrappean low velocity layer (3.2 km/s) with a thickness of about 1.5 km near the shot points SP160, SP180 and SP200. This layer thins out towards north with thicknesses decreasing to 400–800 m which compares well with MT section that shows a conductive layer of a few hundred meter thickness corresponding to the subtrappean Mesozoic sedimentary layer. At the northern edge of the basinal feature the seismic section shows a fault structure which again appears as a well defined linear vertical conductor in MT section (C in Fig. 9) that corresponds to Barwani-Sukta fault. Of the remaining major tectonic faults, while the Narmada South and the Tapti faults find expressions both in the electrical and seismic sections, the southern most Gavligarh fault appears only in the MT model. Further along this traverse the seismic section shows higher crustal velocities (>6.9 km/s) from shallow depths of about 10 km. The MT section also shows relatively conductive (0.002 S/m) lower crustal segments lying below a thinner high resistive upper crustal column.

The MT study has thus brought out several significant subsurface features characterizing the shallow as well as deeper sections of the crust along the Edlabad–Khandwa traverse and compare fairly well with those of the seismic model. Besides these two, i.e., MT and DSS, the NSL region in general is covered by gravity studies (Crumansonata, 1995), which brought out several anomalous features that could be related to subsurface lithology and structure. The MT profile traverses across three such prominent gravity highs, from south to north and these are Jamner high, at the SW end of the traverse, the Burhanpur high in the middle and another major high at the northern end of the traverse. In view of their potential for understanding the subsurface lithology and structure these gravity anomalies may be modeled with constraints from MT and DSS models to get an integrated crustal model. Using the results obtained from MT and considering the available constraints on Moho depths as well as crustal velocity-structure from the deep seismic sounding results (Kaila et al., 1985), an initial model was built to carry out inversion of the gravity data along the traverse. For the purpose of inversion, SAKI (Webring, 1985) package was used. The densities used for Deccan traps, subtrappean sediments, upper and lower crusts and upper mantle are 2.74, 2.67–2.95, 2.4 and 3.30 gm/cm$^3$, respectively. All the primary features that emerged from MT modeling results have been incorporated into the initial models, for each of the inversion trials. The final model obtained is presented in Fig. 12. The model brings out high density crustal blocks at mid to lower crustal levels. Deep seismic sounding results (Kaila et al., 1985) also show that the crustal velocity in this zone is higher, varying from 7 to 7.3 km/s, which agrees well with the density model. The crustal conductors obtained from the MT section (Fig. 9) are seen to be located at the edges of these high density bodies. For example, the two conductive linear features C and B, one covering the sites EK16 to EK18 and the other EK11 to EK12, extending to deeper levels are shown

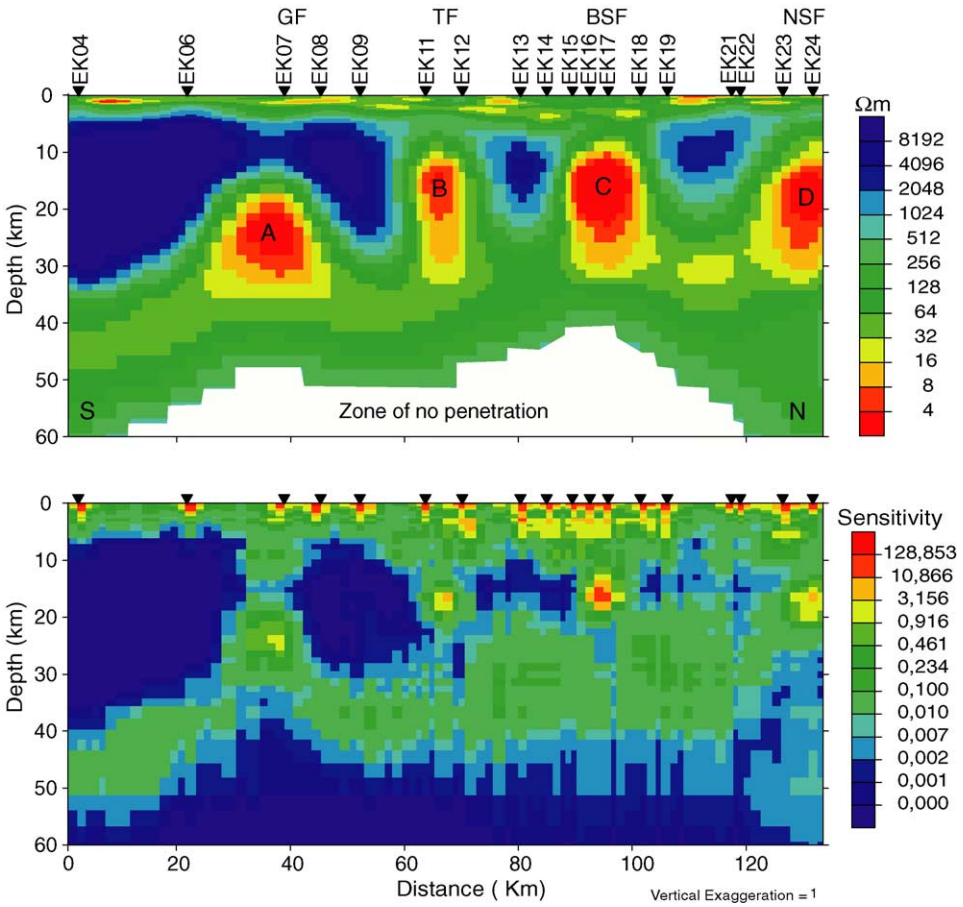


Fig. 9. Deep geoelectric structure obtained from 2D inversion of magnetotelluric data using nonlinear conjugate gradient algorithm of Rodi and Mackie (2001) (top). Sensitivity plot (bottom).

to be connecting to deep seated high density bodies (2.95 gm/cm$^3$). These high density blocks (in the lower crust) correspond to moderately conductive regions in the electrical section (Fig. 9 top) which are relatively less resolved (sensitivity between 0.1 and 1) as could be seen from the sensitivity plot (Fig. 9 bottom). These may be the "source" for the dense and electrically conducting material occupying the fracture zones.

## 6. Origin of high conductivity in the NSL

Occurrence of crustal conductors and there have been several reports on the presence of conductive lower crust in several parts of the world has been a matter of debate for several decades (for e.g., see Jones, 1992 and the references therein). In order to explain the observed high electrical conductivities in the lower continental crust several mechanisms have been proposed (for e.g., see Jones, 1992). Among others, presence of graphite (Glover and Vine, 1992), partial melt (Hermance, 1979, Schilling et al., 1997), hydrated minerals (Stesky and Brace, 1973), metal oxides (Duba et al., 1994; Mareschal et al., 1992) and brines (Hyndman and Shearer, 1989) have been the most commonly cited reasons for the conductive lower crust. Laboratory studies showed that serpentinized rocks exhibit high electrical conductivity (Stesky and Brace, 1973). Glover and Vine (1992, 1994) reported from experimental work that a mid to lower crust composed of am-

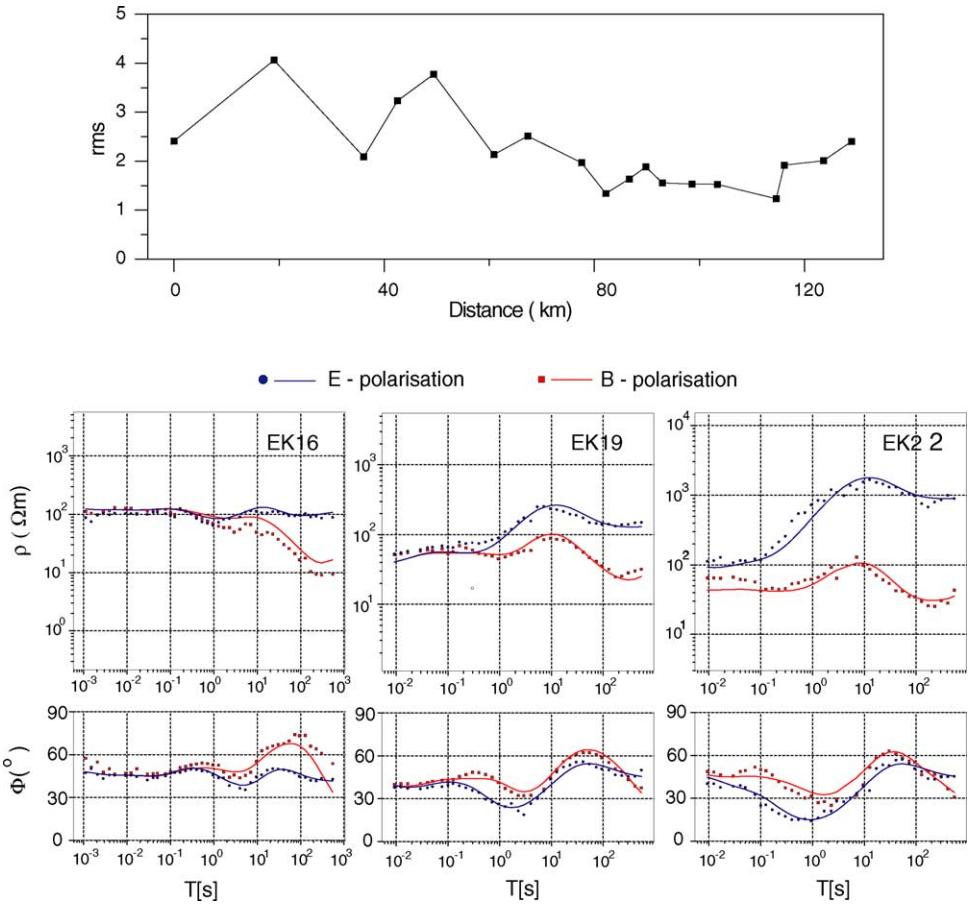


Fig. 10. The rms error along the profile (top). Model fit at few representative sites (bottom).

phibolite saturated with a 0.5 M NaCl shows electrical conductivities sufficient to explain conductivity/depth profiles for the continental crust inferred from geophysical measurements. Roberts and Tyburczy (1999) performed measurements of bulk conductivity of an $Fo_{80}$—basalt partial melt as a function of temperature between 684 and 1244 °C at controlled oxygen fugacity. Melt fraction and compositional variations with temperature calculated using MELTS (Ghiorso and Sack, 1995) indicate that the effect on melt conductivity due to changing melt composition is balanced by change in temperature. They used the electrical conductivity results to estimate melt permeability by adopting a method developed for fluid saturated rocks. Bahr (1997) proposed fractal random networks to explain the conduction mechanism in crustal rocks and scale-dependent electrical anisotropy.

To produce a high electrical conductivity, as observed in the NSL region, a conductive phase probably one (or more) of those discussed above must be present. We have considered each one of these factors to evaluate their significance to explain the high conductivity observed in the NSL region.

### 6.1. *Conducting minerals*

In general silicate and carbonate minerals in the earth's crust have a low electrical conductivity. But electrically conductive source materials that can be found in the Earth's crust include metallic minerals (for e.g., see Jones, 1992). Metallic ore minerals such as iron and copper sulphides have a very high electrical conductivity (100 S/m). While they often occur in discrete ore bodies, they can also occur disseminated over

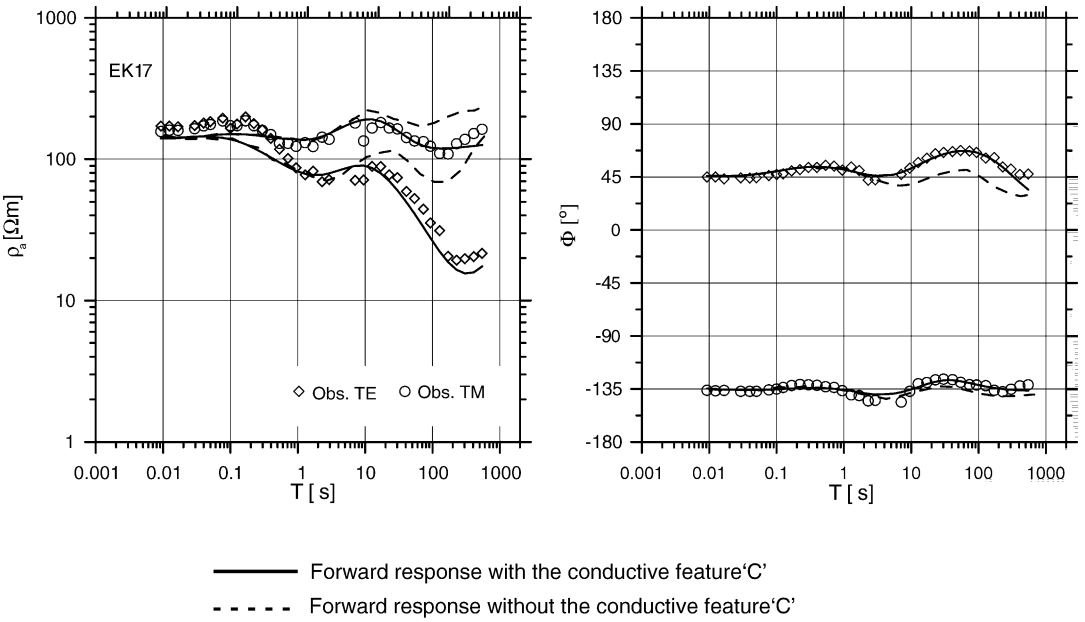


Fig. 11. Test with and with out the conductive feature 'C'.

a larger volume, when they at times become responsible for mid-crustal conductive layers (Li et al., 2003). A large-scale mineral deposit would probably produce detectable gravity and magnetic anomalies. In the absence of evidence for the occurrence of such large-scale mineral resources in this region, we may rule out this factor as a causative source for the high conductivity anomalies observed in this region.

### 6.2. Grain boundary graphite films

Graphite occurs widely in the Earth and exhibits a very high (some times anisotropic) electrical conductivity (Frost et al., 1989; Mareschal, 1990; Joedicke, 1992; Zhamaletdinov, 1996). Graphite is often suggested to be a probable candidate for the high conductivity of the lower crust in the stable continental regions (Frost et al., 1989). However, for graphite to be a conductor, the films must remain connected. Nover et al. (1998) indeed show that connected networks of carbon and ilmenite are responsible for the enhanced crustal conductivity near KTB in Germany. Graphite precipitation along shear planes has been found responsible for many zones of enhanced conductivity in middle curst throughout the world (e.g., ELEKTB Group, 1997). In an active orogen region an interconnected network is unlikely to be stable (Wannamaker, 2000) and graphite is stable only at low oxygen fugacities (Frost et al., 1989). The NSL zone being a part of mobile belt lies in the zone of collision between the Dharwar and Bundelkhand cratons (Radhakrishna and Naqvi, 1986; Radhakrishna, 1989) of Indian peninsular shield and has been tectonically active since Precambrian times. The stability of grain boundary graphite films is thus not certain in such tectonically disturbed regions.

### 6.3. Partial melting

Assuming the high mobility of ions, molten rock is a good electrical conductor. Dry rocks begin to melt at around 1200 °C and this produces a large increase in conductivity The conductivity of pure melt depends on temperature, pressure, the amount of structurally bound and free water and oxygen fugacity (Waff and Weill, 1975; Tyburczy and Waff, 1983). Partial melts in general are associated with low seismic velocity (Schilling et al., 1997). But the high crustal seismic velocity in the NSL region starting from very shallow depths downwards (Kaila et al., 1985) would not go in favour of

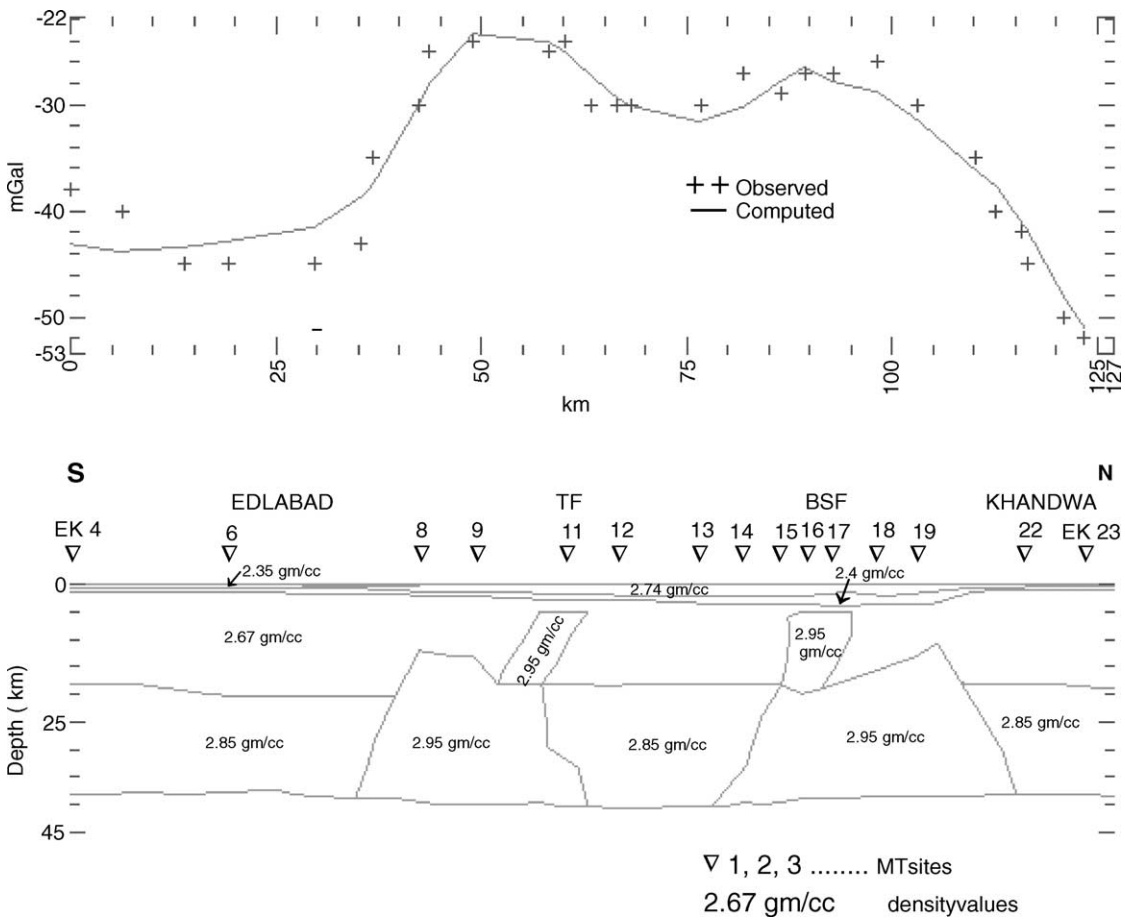


Fig. 12. Density model along Edlabad–Khandwa profile. The primary features obtained from magnetotelluric modeling results have been incorporated into the initial model. Moho depth was constrained from deep seismic sounding results (Kaila et al., 1985).

partial melts as the source of the observed crustal conductors.

### 6.4. Fluids

Lower crustal conducting anomalies were often explained with saline fluids (Hyndman and Hyndman, 1968; Brace, 1971). Several workers invoked the concept of presence of aqueous fluids with a high ionic content to explain the conducting continental lower crust (Shankland and Ander, 1983; Lee et al., 1983). In active subduction zones, at depths less than 40 km a large amount of free water is available from expulsion of pore waters and from $CH_4$–$H_2O$ fluids produced by diagenetic and low-grade metamorphic reactions (Peacock, 1990). In certain cases magma generation in the deep crust by crustal enatexis requires the ingress of external fluids (Wickham and Taylor, 1987).

Coming to the NSL zone, the region besides hosting the conductive features delineated from MT, as discussed before, is also characterized by significant gravity “highs”. To explain the gravity anomalies along the entire NSL region, Singh and Meissner (1995) proposed magmatic underplating with its thickness decreasing from west to east. Venkata Rao (1997) from detailed gravity modeling studies explained the high Bouguer anomaly in the Satpura horst region as magma emplacement in the upper crust in the form of dyke intrusion. The deep seismic sounding results point out to enhanced seismic velocities for the crustal

material at these depths. Further, the NSL zone is generally described as a moderately to high heat flow (70–100 mW/m$^2$) region (Shanker et al., 1991; Roy and Rao, 2000). Taking into account of the gravity modeling results constrained by MT and seismics (Fig. 12), the conductive bodies in the NSL zone are also characterized by increased density and enhanced seismic velocities indicating a more mafic composition of the middle to deep crust consistent with the suggestion of magmatic under plating in the NSL region. Since crustal underplating is often associated with prograde metamorphic processes accompanied by release of fluids that could migrate upwards (for e.g., Hyndman and Shearer, 1989) lowering the resistivities. Hence, presence of fluids in the conductive fault zones at lower crustal depth levels is favoured. Considering the upper Hashin–Shtrikman bound with resistivities of 0.3 Ω m for the conductive phase and $10^3$ Ω m for the resistive phase, 3–7% of interconnected pore space is required to yield an effective resistivity of ∼5 Ω m which falls with in the resistivites (3–30 Ω m) observed in the conductors.

All these evidences point out that the crustal electrical conductors delineated from MT results in the NSL region may be attributed to mafic material associated with fluids that could have come from underplating of the lower crust in this region.

## 7. Conclusions

1. MT modeling results brought out four high conductive structural features extending from mid to deep crustal levels. These are interpreted as the electrical signatures of the geologically mapped major tectonic faults namely, the Gavligarh, Tapti, Barwani-Sukta and Narmada South faults.
2. A major subtrappean sedimentary basinal feature has been delineated in the northern end of the traverse.
3. The integrated modeling results show that, in the segment of the traverse between EK8 and EK22, the lower crust is characterized by two blocks of relatively higher density material (2.95 gm/cm$^3$). These blocks are moderately conductive (50–500 Ω m) and correspond to the regions of enhanced seismic velocity (7–7.3 km/s).
4. The conductive features (3–30 Ω m) at mid to lower crustal depths as also the lower crustal column, characterized by high density and high seismic velocity are interpreted to be due to presence of mafic material associated with fluids due to crustal underplating of the NSL region.
5. In the hypocentral regions of the two earthquakes namely, the 6.0 M 1997 Jabalpur earthquake and Khandwa swarm seismic activity during 1998, the electrical structure is characterized by highly conductive subsurface medium. It may be inferred that heterogeneities associated with such anomalous mid-lower crustal lithologies in the NSL zone facilitate development of conditions suitable for generation of seimotectonic activity at the major deep faults in this region.

## Acknowledgements

The research was supported by grant ESS/CA/A8-06/94 from Department of Science and Technology (DST), Government of India. We thank Michael Becken for providing the MT tensor analysis code and for many useful discussions. Thanks to Director, NGRI for permitting to publish this work. We are extremely thankful to Heinrich Brasse for constructive suggestions and the facilities extended to BPKP during his stay at Freie Universitat (FU) Berlin. We thank both the reviewers, Karsten Bahr and A. Gatzemeier for many constructive suggestions, which helped improving the manuscript. B. Prasanta K. Patro thanks DST for BOYSCAST fellowship to FU Berlin.

## References

Acharya, S.K., Kayal, J.R., Roy, A., Chaturvedi, R.K., 1998. Jabalpur earthquake of May 22, 1997: constraint from aftershock study. J. Geol. Soc. India 51, 195–304.

Arora, B.R., Waghmare, S.Y., Mahashabde, M.V., 1995. Geomagnetic depth sounding along Hirapur–Mandla–Bhandre profile, central India. In: Sinha Ray, S., Gupta, K.R. (Eds.), Continental Crust of NW and Central India. Geological Society of India, pp. 519–535 (Mem. No. 31).

Auden, J.B., 1949. Geological discussion of the Satpura hypothesis. Proc. Natl. Inst. Sci. India 15, 315–340.

Bahr, K., Bantin, M., Jantos, E., Schneider, E., Storz, W., 2000. Electrical anisotropy from electromagnetic array data: implications

for the conduction mechanism and for distortion at long periods. Phys. Earth Planet. Int. 119, 237–257.
Becken, M., Burkhardt, H., 2004. An ellipticity criterion in magnetotelluric tensor analysis. Geophys. J. Int. 159, 69–82.
Bahr, K., 1988. Interpretation of the magnetotelluric impedance tensor: regional induction and local telluric distortion. J. Geophys. 62, 119–127.
Bhar, K., 1991. Geological noise in magnetotelluric data: a classification of distortion types. Phys. Earth Planet. Int. 66, 24–38.
Bahr, K., 1997. Electrical anisotropy and conductivity distribution functions of fractal random networks and of the crust: the scale effect of connectivity. Geophys. J. Int. 130, 649–660.
Brace, W.F., 1971. Resistivity of saturated crustal rocks to 40 km based on laboratory measurements. In: Heacock, J.G. (Ed.), Structure and Physical Properties of the Earth's Crust, vol. 14. AGU Geophys. Monogr. Ser., pp. 206–210.
Brasse, H., Lezaeta, P., Rath, V., Schwalenberg, K., Soyer, W., Haak, V., 2002. The Bolivian Altiplano conductivity anomaly. J. Geophys. Res. 107, doi:10.1029/2001JB00391.
Crumansonata, 1995. Geoscientific Studies of the Son–Narmada–Tapati Lineament Zone. Geological Society of India. Special Publication 10,371.
Duba, A.G., Heikamp, S., Meureer, W., Nover, G., Will, G., 1994. Evidence from borehole samples for the role of accessory minerals in lower crustal conductivity. Nature 367, 59–61.
ELEKTB Group, 1997. KTB and the electrical conductivity of the crust. J. Geophy. Res. 102, 18289–18306.
Frost, B.R., Fyfe, W.S., Tazaki, K., Chan, T., 1989. Grain-boundary graphite in rocks and implications for high electrical conductivity in the lower crust. Nature 340, 134–136.
Ghiorso, M.S., Sack, R.O., 1995. Chemical mass transfer in magmatic processes. IV. A revised and internally consistent thermodynamic model for the interpolation and extrapolation of liquid–solid equilibria in magmatic systems at elevated temperatures and pressures. Contrib. Mineral. Petrol. 119, 197–212.
Glover, P.W.J., Vine, F.J., 1992. Electrical conductivity of carbon bearing granulite at raised temperatures and pressures. Nature 3609, 723–726.
Glover, P.W.J., Vine, F.J., 1994. Electrical conductivity of the continental crust. Geophys. Res. Lett. 21, 2357–2360.
Gokarn, S.G., Rao, C.K., Gupta, G., Singh, B.P., Yamashita, M., 2001. Deep crustal structure in central India using magnetotelluric studies. Geophys. J. Int. 144, 685–694.
Gupta, M.L., Sukhija, B.S., 1974. Preliminary studies of some geothermal areas in India. Geothermics 3, 105–112.
Hansen, P.C., 1998. Rank Deficient and Discrete Ill-Posed Problems, Numerical Aspects of Linear Inversion. SIAM, Philadelphia.
Heise, W., Pous, J., 2001. Effects of anisotropy on the two-dimensional inversion procedure. Geophys. J. Int. 147, 610–621.
Hermance, J.F., 1979. The electric conductivity of materials containing partial melts: a simple model from Archie's law. Geophys. Res. Lett. 6, 613–616.
Hyndman, R.D., Shearer, P.M., 1989. Water in the lower continental crust: modeling magnetotelluric and seismic reflection results. Geophys. J. Int. 98, 343–365.
Hyndman, R.D., Hyndman, D.W., 1968. Water saturation and high electrical conductivity in the lower crust. Earth Planet. Sci. Lett. 4, 427–432.
Joedicke, H., 1992. Water and graphite in the Earth's Crust—an approach to interpretation of conductivity models. Surv. Geophys. 13, 381–407.
Jones, A.G., 1992. Electrical conductivity of the continental lower crust. In: Fountain, D.M., Arculus, R., Key, R.W. (Eds.), Continental Lower Crust. Elsevier, Amsterdam, pp. 81–143.
Kaila, K.L., Reddy, P.R., Dixit, M.M., Koteswar Rao, P., 1985. Crustal structure across the Narmada–Son lineament, Central India from deep seismic soundings. J. Geol. Soc. India 26, 465–480.
Kailasam, L.N., 1979. Plateau uplift in Peninsular India. Tectonophysics 61, 243–269.
Krishnan, M.S., Swaminath, J., 1959. The great Vindhyan basin of northern India. J. Geol. Soc. India 1, 10–30.
Lee, C.D., Vine, F.J., Ross, R.G., 1983. Electrical conductivity models for the continental crust based on laboratory measurements on high-grade metamorphic rocks. Geophys. J. R. Astron. Soc. 72, 353–371.
Li, S., Unsworth, M.J., Booker, J.R., Wei, W., Tan, H., Jones, A.G., 2003. Partial melt or aqueous fluid in the mid-crust of Southern Tibet? Constraints from INDEPTH Magnetotelluric data. Geophys. J. Int. 153, 289–304.
Mareschal, M., 1990. Electrical conductivity: the story of an elusive parameter and how it possibly relates to the Kapuskasing Uplift (LITHOPRPBE Canada). In: Salisbury, M.H., Fountain, D.M. (Eds.), Exposed Cross-sections of the Continental Crust. Kulwer, Dordrecht, pp. 453–468.
Mareschal, M., Fyfe, W.S., Percival, J., Chan, T., 1992. Grain boundary graphite and Kapuskasing gneisses and implications for lower crustal conductivity. Nature 357, 674–676.
Mishra, P.C., Srirama, P., Nautiyal, S.C., Datttatreyam, R.S., Suresh, G., Bhattacharya, S.N., 2001. A seismotectonic evaluation of Pandhana swarm activity in Satpura block Khandwa-Khargone belt, Madhya Pradesh. In: Proceedings of the International Conference on Seismic Hazard with Particular Reference to Bhuj Earthquake of January 26, 2001, Abstract volume, pp. 362–364.
Nover, G., Heikamp, S., Meurer, H.J., Freund, D., 1998. In-situ electrocal conductivity and permeability of mid-crustal rocks from the KTB drilling: consequences for high conductive layers in the Earth crust. Surv. Geophys. 19, 73–85.
Patro, B.P.K., 2002. A magnetotelluric study of crustal geoelectric structure in western India in relation to seismotctonics of the Deccan trap region. Ph.D. thesis. Osmania University, Hyderabad.
Peacock, S.M., 1990. Fluid processes in subduction zones. Science 248, 329–337.
Radhakrishna, B.P., 1989. Suspect tectono-stratigraphic terrane elements in the Indian subcontinent. J. Geol. Soc. India 34, 1–24.
Radhakrishna, B.P., Naqvi, S.M., 1986. Precambrian continental crust of India and its evolution. J. Geol. 94, 145–166.
Rao, C.K., Gokarn, S.G., Singh, B.P., 1995. Upper crustal structure in the Torni-Purnad region, Central India using magnetotellurics studies. J. Geom. Geolel. 47, 411–420.

Rao, C.K., Ogawa, Y., Gokarn, S.G., Gupta, G., 2004. Electromagnetic imaging of magma across the Narmada Son lineament, central India. Earth Planets Space 56, 229–238.

Rao, A.P., Venkateswarulu, P.D., Rao, K.J., Kamaraju, M.V.V., 1982. Report on the geophysical investigations under CRUMANSONATA project in the Bagh area, Dhar district, M.P. Unpublished Progress Report of the GSI for FS, pp. 79–80.

Rao, K.V., Sastry, P.R., 1986. A geophysical investigation along Kanti-Nagpur traverse under project CRUMANSONTATA. Unpublished Report GSI, CR.

Rastogi, B.K., 1997. Seismo-tectonics along Narmada–Son rift zone. In: Proceedings of workshop on the tectonics of Narmada–Son lineament, #####, pp. 37–49.

Roberts, J.J., Tyburczy, J.A., 1999. Partial-melt electrical conductivity: Influences of melt composition.(Misc. Publ. No. 63), J. Geophys. Res. 104, 7055–7065.

Rodi, W., Mackie, R.L., 2001. Nonlinear conjugate gradients algorithm for 2-D magnetotelluric inversion. Geophysics 66, 174–187.

Roy, S., Rao, R.U.M., 2000. Heat flow in the Indian shield. J. Geophys. Res. 105, 25587–25604.

Sarma, S.V.S., Nagarajan, N.N., Someswara Rao, M., Harinarayana, T., Virupakshi, G., Murty, D.N., Sarma, M.V.C., Gupta, K.R.B., 1996. Geo-electric signatures of crustal reactivation in Central India—a magnetotelluric study. In: Proceedings of the 2nd International Seminar and Exhibition, AEG, SG-21, pp. 206–207.

Schilling, F.R., Partzsch, G.M., Brasse, H., Schwarz, G., 1997. Partial melting below the magmatic arc in the central Andes deduced from geoelectromagnetic field experiments and laboratory data. Phys. Earth Planet. Int. 103, 17–31.

Shanker, R., 1988. Heat flow map of India and discussions on its geological and economic significance. Ind. Miner. 42 (2), 89–110.

Shanker, R., Guha, S.K., Sethi, N.N., Muthuraman, K., 1991. Gerothermal Atlas of India, GSI, Geological Survey of India, Spec. Publ. 19, p. 144.

Shankland, T.J., Ander, M.E., 1983. Electrical conductivity, temperatures, and fluids in the lower crust. J. Geophys. Res. 88, 9475–9484.

Singh, A.P., Meissner, R., 1995. Crustal configuration of the Narmada–Tapti region (India) from gravity studies. J. Geodyn. 20, 111–127.

Smith, J.T., Booker, J.R., 1991. Rapid inversion of two and three dimensional magnetotelluric data. J. Geophys. Res. 96, 3905–3922.

Smith, J.T., 1995. Understanding telluric distortion matrices. Geophys. J. Int. 122, 219–226.

Smith, J.T., 1997. Estimating galvanic-distortion magnetic fields in magnetotellurics. Geophys. J. Int. 130, 65–72.

Stesky, R.S., Brace, W.F., 1973. Electrical conductivity of serpentinised rocks to 6 kbars. J. Geophys. Res. 78, 7614–7621.

Swift Jr., C.M., 1967. A magnetotelluric investigations of electrical conductivity anomaly in the southwestern United States. Ph.D. thesis, MIT.

Ting, S.C., Hohmann, G.W., 1981. Integral equation modeling of three-dimensional magnetotelluric response. Geophysics 46, 182–197.

Tyburczy, J.A., Waff, H.S., 1983. Electrical conductivity of molten basalt and andesite to 25 kbar pressure: geophysical significance and implications for charge transport and melt structure. J. Geophys. Res. 88, 2413–2430.

Venkata Rao, K., 1997. Paleomagma chamber in the upper crust—plaussible secondary source for Deccan basalts of the Satpura region in central India. J. Geol. Soc. India 50, 673–680.

Verma, R.K., Banerjee, P., 1992. Nature of continental crust along the Narmada–Son-Lineament inferred from gravity and deep seismic sounding data. Tectonophysics 202, 375–397.

Waff, H.S., Weill, D.F., 1975. Electrical conductivity of magmatic liquids: effects of temperature, oxygen fugacity and composition. Earth Planet. Sci. Lett. 28, 254–260.

Wannamaker, P.E., 2000. Comments on “The petrologic case for a dry lower crust” by Bruce W.D. Yardley and John W. Valley. J. Geophys. Res. 105, 6057–6064.

Webring, M., 1985. Semi-automatic Marquardt inversion of gravity and magnetic traverses (SAKI), U.S. Geological Survey Open-file Report, pp. 85–122 (USGS).

West, W.D., 1962. The line of Narmada–Son Valley. Curr. Sci. 31, 43–144.

Wickham, S.M., Taylor, H.P.J., 1987. Stable isotope constraints on the origin and depth of penetration of hydrothermal fluids associated with Hercynian regional metamorphism and crustal anatexis in the Pyrenees.

Zhamaletdinov, A.A., 1996. Graphite in the Earth’s crust and electrical conductivity anomalies, Izvestiya. Phys. Solid Earth. 32, 272–288.